Diazonium Ions. A Theoretical Study of Pathways to Automerization, Thermodynamic Stabilities, and Topological Electron Density Analysis of the Bonding

Rainer Glaser

Department of Chemistry, Yale University, New Haven, Connecticut 06511[1] *(Received: March 7, 1989; In Final Form: May 22, 1989)*

Equilibrium geometries and transition-state structures for automerization and thermodynamic stabilities toward loss of N_2 and N scrambling are reported for the parent alkyl-, alkenyl-, and alkynyldiazonium ions $[RN_2]^+$ (R = methyl (**1**), vinyl (**2**), and ethynyl (**3**)). The automerizations of **1** and **2** involve essentially complete disconnection, rotation, and reconnection of N_2, but N scrambling in **3** occurs within a bound ion–molecule complex via a two-step process. The degree of unsaturation affects the binding energies in an unexpected fashion; they increase in the order **2** < **1** < **3**. This finding has led to important conclusions regarding the electronic structures of vinyl cations. Topological electron density of the classical vinyl cation shows *CC-π-density localization* at the CH group and a large positive charge for the CH_2 group. This result is supported by *structural* features of β-disubstituted vinyl cations, and it provides a consistent explanation for the lability of **2**, for the higher stability of β-(di)substituted alkenyldiazonium ions, and for the C_β-S_N2t-type chemistry of the latter. Density integration shows *small* charges (<+0.16) for the diazo groups in **1**–**3**. Electron density accumulation in the CN-bonding region, strong internal polarization of N_2, and radial expansion of the density in the NN-bonding region are common features of the electron density distributions of **1**–**3**. These features are explained with a bonding model invoking synergetic σ-donation from N_2 to the positively charged hydrocarbon fragment and π-back-donation of comparable magnitude. Implications are discussed regarding the site of nucleophilic attack, the electronic structures of heterosubstituted diazonium ions, and the possibility of stabilizing P_2 in diphosphonium ions. Of theoretical interest are the occurrences of nonnuclear (3,–3) and noncage (3,+3) critical points in CC triple bonds. The crucial role of the curvature λ_3 is emphasized as a parameter for the partitioning of multiple bonds with low polarities.

Introduction

Alkyldiazonium ions are highly reactive intermediates in the nitrosation of primary amines, the acid decomposition of 3-alkyl-1-aryltriazenes, and in decomposition reactions of *N*-nitrosoamides and related compounds.[3] All of these substrates are known to be potent carcinogens, and alkyldiazonium ions have frequently been invoked as the reactive electrophilic species responsible for mutagenic modification of cellular constituents, and specifically the alkylation of DNA.[4-8] The transient character of alkyldiazonium ions has made it difficult to characterize these important intermediates by physical techniques. Alkyldiazonium ions have only been observed in superacid media in a few instances.[9] Methyldiazonium ions has been generated under ion cyclotron conditions, and its gas-phase reactions have been studied.[10,11] In the solid state alkyldiazonium ions can only be stabilized by complexation to transition metals.[12] In these complexes the alkyldiazonium ligands are bent and they clearly differ greatly from the free species. A variety of alkenyldiazonium salts are known, and their thermal stabilities toward loss of N_2 varies greatly.[13-15] Alkenyldiazonium ions with alkyl substituents in the β-position(s) usually eliminate N_2 spontaneously, but alkenyldiazonium ions with β-heterosubstituents are rather stable toward dediazoniation.[13] The chemistry of the latter is characterized primarily by C_β-S_N2t-type chemistry rather than vinyl cation chemistry.[16,17] Phenylethynyldiazonium salts[18] represent the first examples of compounds with C-sp-attached diazonium functions.[19] Solvolytic dediazoniation of these salts proceeds primarily via the vinyldiazonium ion, not by S_N1 reaction. Theoretical studies have shown that the unimolecular, thermal dediazoniation of the parent ethynyldiazonium is greatly endothermic and also kinetically hindered.[20-22]

(1) (a) Part of this work was carried out in the Department of Chemistry, University of California, Berkeley. (b) Permanent address: Department of Chemistry, University of Missouri—Columbia, Columbia, MO 65211.

(2) Presented in part at the 195th National Meeting of the American Chemical Society, Toronto, Ontario, Canada, June 1988.

(3) Review: Kirmse, W. *Angew. Chem., Int. Ed. Engl.* **1976**, *15*, 251.

(4) For reviews see: *Chemical Carcinogens, Vol. 2*; Searle, Ch. E., Ed.; ACS Monograph 182; American Chemical Society, Washington, DC, 1984; Chapters 12–14.

(5) Smith, R. H.; Koepke, S. R.; Tondeur, Y.; Denlinger, C. L.; Michejda, C. L. *J. Chem. Soc., Chem. Commun.* **1985**, 936.

(6) (a) Sullivan, J. P.; Wong, J. L. *Biochim. Biophys. Acta* **1977**, *479*, 1. (b) Yuspa, S. H.; Poirier, M. C. *Adv. Cancer Res.* **1987**, *50*, 25.

(7) For studies of the reactions of aryldiazonium ions with adenine and guanine, see: (a) Chin, A.; Hung, M.-H.; Stock, L. M. *J. Org. Chem.* **1981**, *46*, 2203. (b) Hung, M.-H.; Stock, L. M. *J. Org. Chem.* **1982**, *47*, 448.

(8) (a) Hopfinger, A. J.; Mohammad, S. N. *J. Theor. Biol.* **1980**, *87*, 401. (b) Ford, G. P.; Scribner, J. D. *J. Am. Chem. Soc.* **1983**, *105*, 349.

(9) (a) Mohrig, J. R.; Keegstra, K. *J. Am. Chem. Soc.* **1967**, *89*, 5492. (b) Mohrig, J. R.; Keegstra, K.; Maverick, A.; Roberts, R.; Wells, S. J. *J. Chem. Soc., Chem. Commun.* **1974**, 780. (c) Avaro, M.; Levisalles, J.; Sommer, J. M. *J. Chem. Soc., Chem. Commun.* **1968**, 410. (d) McGarrity, J. F.; Cox, D. Ph. *J. Am. Chem. Soc.* **1983**, *105*, 3961.

(10) (a) Foster, M. S.; Beauchamp, J. L. *J. Am. Chem. Soc.* **1972**, *94*, 2425. (b) Foster, M. S.; Williamson, A. D.; Beauchamp, J. L. *Int. J. Mass. Spectrom. Ion Phys.* **1974**, *15*, 429.

(11) McMahon, T. B.; Heinis, T.; Nicol, G.; Hovey, J. K.; Kebarle, P. *J. Am. Chem. Soc.* **1988**, *110*, 7591.

(12) (a) $CpM(CO)_2(N_2CH_2Si(CH_3)_3)$ (M = Mo, W): Lappert, M. F.; Poland, J. S. *J. Chem. Soc., Chem. Commun.* **1969**, 1061. (b) $MoI(N_2CH_3)(dppe)_2$ (dppe = 1,2-bis(diphenylphosphino)ethane): Day, V. W.; George, T. A.; Iske, S. D. A. *J. Am. Chem. Soc.* **1975**, *97*, 4127. (c) $CpW(CO)_2N_2CH_3$: Herrmann, W. A. *Angew. Chem., Int. Ed. Engl.* **1975**, *14*, 355. Hillhouse, G. L.; Haymore, B. L. *Inorg. Chem.* **1979**, *18*, 2423. (d) $CH_3N_2[Mn(CO)_4]$: Herrmann, W. A.; Ziegler, M. L.; Weidenhammer, K. *Angew. Chem., Int. Ed. Engl.* **1976**, *15*, 368.

(13) (a) Bott, K. *Chem. Ber.* **1975**, *108*, 402. (b) Bott, K. *Angew. Chem., Int. Ed. Engl.* **1979**, *18*, 259. (c) Bott, K. *Alkenediazonium Compounds in The Chemistry of Functional Groups, Suppl. C*; Patai, S., Rappoport, Z., Eds.; Wiley: New York, 1983; p 671. (d) Bott, K. *Tetrahedron Lett.* **1985**, *26*, 3199.

(14) Reimlinger, H. *Angew. Chem.* **1963**, *75*, 788.

(15) (a) Curtin, D. Y.; Kampmeier, J. A.; O'Connor, R. *J. Am. Chem. Soc.* **1965**, *87*, 863. (b) Newman, M. S.; Weinberg, A. E. *J. Am. Chem. Soc.* **1956**, *78*, 4654. (c) Newman, M. S.; Beard, C. D. *J. Am. Chem. Soc.* **1970**, *92*, 7564. (d) Jones, W. N.; Miller, F. W. *J. Am. Chem. Soc.* **1967**, *89*, 1960.

(16) Review: Stang, P. J.; Rappoport, Z.; Hanack, M.; Subramanian, L. R. *Vinyl Cations*; Academic Press: New York, 1979.

(17) For synthetic applications of alkenyldiazonium ions, see: Saalfrank, R. W.; Weiss, B.; Peters, K.; Schnering, H. G. v. *Chem. Ber.* **1985**, *111*, 4026, and references therein.

(18) (a) Helwig, R.; Hanack, M. *Chem. Ber.* **1985**, *118*, 1008. (b) Hanack, M.; Vermehren, J., private communication.

(19) For the synthesis of diaminocyclopropeniumyldiazonium salts, formally C-sp-attached diazonium dication systems, see: Weiss, R.; Wagner, K.-G.; Priesener, C.; Macheleid, J. *J. Am. Chem. Soc.* **1985**, *107*, 4491.

0022-3654/89/2093-7993$01.50/0

TABLE I: Symmetry Properties, Character, Vibrational Zero-Point Energies, and Energies

molecule[a]	no.	PG[b]	DOF[c]	CSS[d]	VZPE[e]	energies[f] RHF	MP2	MP3	MP4[DQ]	MP4[SDQ]
methyldiazonium ion										
end-on	**1a**	C_{3v}	4	M	27.64	148.216 06[g]	148.645 85[g]	148.653 68[g]	148.660 11	148.665 31
edge-on, staggered	**1b**	C_s	7	TS	23.77	148.177 47	148.580 22	148.593 07	148.599 72	148.604 13
edge-on, eclipsed	**1c**	C_s	8	SOSP	23.75	148.177 47	148.580 22	148.593 07	148.599 72	148.604 13
vinyldiazonium ion										
end-on	**2a**	C_s	11	M	30.83	186.059 35	186.608 80	186.619 55	186.625 31	186.632 31
edge-on, in plane	**2b**	C_s	11	TS	25.52	186.031 48	186.556 88	186.574 55	186.580 90	186.588 78
edge-on, out of plane	**2c**	C_s	10	SOSP	25.41	186.030 93	186.555 97	186.573 76	186.580 07	186.587 94
ethynyldiazonium ion										
end-on	**3a**	$C_{\infty v}$	4	M	17.11	184.797 72	185.350 24	185.346 46	185.350 83	185.359 21
edge-on	**3b**	C_{2v}	4	M	14.88	184.711 84	185.260 22	185.264 92	185.265 11	185.274 63
edge-on, asymmetric	**3c**	C_s	7	TS	14.82	184.703 11	185.250 05	185.252 54	185.255 16	185.265 10
dinitrogen		$D_{\infty h}$			3.55[h]	108.943 95	109.248 08	109.245 27	109.249 30	109.253 14
methyl cation		D_{3h}			19.04[h]	39.230 64	39.325 14	39.341 58	39.344 33	39.344 67
vinyl cation, classical		C_{2v}			21.55[h]	77.086 73	77.306 57	77.327 46	77.329 75	77.333 74
vinyl cation, distorted[i]		C_s				77.022 35	77.253 14	77.272 19	77.274 67	77.279 81
ethynyl cation[j]		$C_{\infty v}$			8.73[h]	75.785 55	75.940 89	75.960 08	75.962 23	75.965 97

[a] Compare Figures 1–3. [b] Symmetry point group. [c] Degrees of freedom. [d] Character of the stationary structure: M, minimum; TS, transition-state structure; SOSP, second-order saddle-point structure. [e] Vibrational zero-point energies (RHF/6-31G*) are scaled (factor 0.9). [f] Energies ($-E$) in atomic units. Møller–Plesset calculations were carried out at MPx(fc)/6-31G*//RHF/6-31G*. [g] Reference 39. [h] See ref 20. [i] Distorted vinyl cation. Optimal C_s structure (angstroms and degrees) with a fixed (C–C–H1) angle of 120° (H2 and H1 are cisoid): C–C 1.2701, C1–H1 1.0885, C2–H2 1.0999, C2–H3 1.0747, H2–C2–C1 98.912, H3–C2–C1 139.923. [j] Calculated in its ground state $^3\Pi$ using the UHF formalism; cf. ref 20 and text.

Knowledge about the electronic structures of the diazonium ions is pertinent to more fully understand their chemistry. In solution the properties of the diazonium systems certainly are affected by primary solvation and ion association,[23] and their understanding requires prior detailed studies of the diazonium ions themselves. Here the results are reported of a theoretical study of the prototypical diazonium ions with C-sp^3-, C-sp^2-, or C-sp-attached diazo functions. Specifically, the potential energy surfaces of methyl-, vinyl-, and ethynyldiazonium ions have been explored in order to study the effects of unsaturation of the hydrocarbon fragment on thermodynamic stabilities and electronic structures. Thermodynamic stabilities are discussed with respect to unimolecular dediazoniation as well as automerization.[24] Electronic structures are analyzed with the topological method of Bader and co-workers.[25] The usual Lewis notations are found to be inadequate for all of the diazonium ions. A model for CN bonding is proposed which is compatible with the topological features of the electron densities. Important implications are discussed concerning the reactivities of diazonium ions, the electronic structures of vinyl cations, and the possibility of stabilizing diphosphorus in diphosphonium cations.

Computational Aspects

Ab initio calculations were carried out with the program Gaussian90 and earlier versions.[26] Geometry optimizations[27] were performed under the constraints of the symmetry point groups specified. The Hessian matrix and harmonic vibrational frequencies were calculated analytically to characterize stationary structures as minima, transition-state structures, or second-order saddle points, and to obtain vibrational zero-point energies (VZPEs). Since vibrational frequencies and VZPEs generally are overestimated at this computational level,[28] zero-point-energy corrections to relative energies and reaction energies were scaled (factor 0.9) unless otherwise noted. In general, optimization and characterization of stationary structures were carried out with restricted Hartree–Fock (RHF) wave functions and with the 6-31G* basis set.[29] In a few cases the basis set 6-311G** and 6-311++G** were used.[30] The RHF/6-31G* wave functions were transformed into a format suitable for the electron density analysis with the program Psichk.[31] Topological properties of the electron densities were determined with the program Extreme.[32] The program Proaims[33] was used to determine fragment

TABLE II: Thermodynamic Stabilities[a,b]

molecule	RHF	MP2	MP3	MP4 DQ	MP4 SDQ
1a	21.0	40.5	36.9	36.7	37.3
1b,c	0.6	3.2	2.7	2.6	2.8
2a	12.3	28.3	23.7	23.3	22.8
2b	0.1	1.0	0.7	0.7	0.8
2c	−0.2	0.5	0.3	0.3	0.4
3a	38.0	96.3	83.6	82.5	83.0
3b	−13.7	42.1	34.8	31.0	32.2
3c	−19.1	35.8	27.1	24.8	26.3

[a] The energies for the dediazoniation reactions **1** → $CH_3^+ + N_2$, **2** → $C_2H_3^+ + N_2$, and **3** → $HCC^+(^3\Pi) + N_2$ in kcal/mol. Values include scaled (factor 0.9) vibrational zero-point energies (Table I). [b] MPx-(fc)/6-31G*//RHF/6-31G*.

(20) Glaser, R. *J. Am. Chem. Soc.* **1987**, *109*, 4237.
(21) Hanack, M.; Vermehren, J.; Helwig, R.; Glaser, R. *Stud. Org. Chem. (Amsterdam), Phys. Org. Chem.* **1987**, *31*, 17.
(22) Angelini, G.; Hanack, M.; Vermehren, J.; Speranza, M. *J. Am. Chem. Soc.* **1988**, *110*, 1298.
(23) The reactions of methyldiazonium ions in solution are affected by ion association ("nitrogen separated ion pairs"): (a) Gold, B.; Deshpande, A.; Linder, W.; Hines, L. *J. Am. Chem. Soc.* **1984**, *106*, 2072. (b) Bredereck, H.; Sieber, R.; Kampkenckel, L. *Chem. Ber.* **1956**, *89*, 1169. (c) Cf. ref 6a.
(24) Automerization: *terminus technicus* for an isomerization in which reagent and product are indistinguishable.
(25) (a) Bader, R. F. W. *Acc. Chem. Res.* **1985**, *18*, 9. (b) Bader, R. F. W.; Nguyen-Dang, T. T.; Tal, Y. *Rep. Prog. Phys.* **1981**, *44*, 893.
(26) Gaussian90, Development Version (Release A); Frisch, M. J.; Head-Gordon, M.; Schlegel, H. B.; Raghavachari, K.; Binkley, J. S.; Gonzales, C.; Defrees, D. J.; Fox, D. J.; Whiteside, R. A.; Seeger, R.; Melius, C. F.; Baker, J.; Martin, R. L.; Kahn, L. R.; Stewart, J. J. P.; Fluder, E. M.; Topiol, S.; Pople, J. A.; Gaussian, Inc., Pittsburgh, PA, 1988.
(27) Schlegel, H. B. *J. Comput. Chem.* **1982**, *3*, 214.
(28) Francl, M. M.; Pietro, W. J.; Hehre, W. J.; Binkley, J. S.; Gordon, M. S.; DeFrees, D. J.; Pople, J. A. *J. Chem. Phys.* **1982**, 77, 3654, and references therein.
(29) (a) Hehre, W. J.; Ditchfield, R.; Pople, J. A. *J. Chem. Phys.* **1972**, *56*, 2257. (b) Hariharan, P. C.; Pople, J. A. *Theor. Chim. Acta* **1973**, *28*, 213. (c) Reference 28. (d) Six Cartesian second-order Gaussians were used for d shells.
(30) (a) Krishnan, R.; Binkley, J. S.; Seeger, R.; Pople, J. A. *J. Chem. Phys.* **1980**, *72*, 650. (b) Five pure d orbitals were used. (c) Diffuse functions: Clark, T.; Chandrasekhar, J.; Spitznagel, G. W.; Schleyer, P. v. R. *J. Comput. Chem.* **1983**, *4*, 294.
(31) LePage, T. J. Yale University, New Haven, CT, 1988.
(32) Biegler-König, F. W. McMaster University, Hamilton, Ontario, 1980.
(33) (a) Biegler-König, F. W.; Duke, F. A. McMaster University, Hamilton, Ontario, 1981. (b) Modified by Lau, C. D. H. McMaster University, Hamilton, Ontario, 1983. (c) Adapted for a CSPI array processor by LePage, T. J. Yale University, New Haven, CT, 1987.

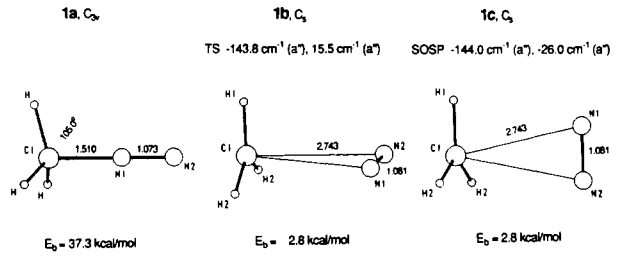

Figure 1. C-sp³-attached diazonium function: methyldiazonium ion (**1**). Molecular-model-type drawings of stationary structures of **1** as calculated at the RHF/6-31G* level. Energies E_b (in kcal/mol) for reactions **1** → $CH_3^+ + N_2$ are those determined at the MP4[SDQ]/6-31G*//RHF/6-31G* level, and they include vibrational zero-point-energy corrections. Frequencies of imaginary vibrational modes are given to characterize higher order stationary structures.

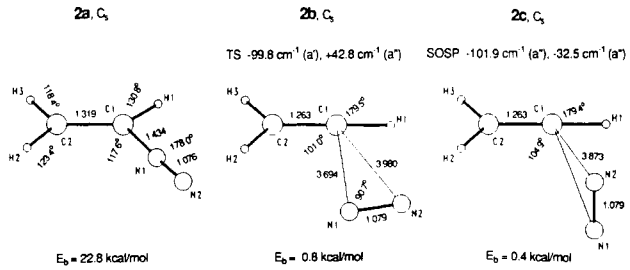

Figure 2. C-sp²-attached diazonium function: vinyldiazonium ion (**2**). Compare legend to Figure 1.

populations and stabilities by density integration techniques[34] defined by the theory of atoms in molecules.[25] In general, energies were calculated with the RHF/6-31G* geometries at levels of Møller–Plesset perturbation theory[35] up to MP4[SDQ]/6-31G* in the frozen-core approximation to account, in part, for electron correlation.

Computations were carried out on DEC MicroVax II workstations, a DEC Vax-11/750, the DEC Vax-8600 at the Berkeley Campus Computer Facility, the Multiflow Trace 7 minisupercomputer at the Yale Chemistry Department, and on the CRAY II at the Pittsburgh Supercomputing Center. Electron density analyses were carried out using a MAP CSPI array processor hosted by a Microvax II workstation.

Results and Discussion

1. Dediazoniation and Automerization. Total energies and thermodynamic stabilities of methyl- (**1**), vinyl- (**2**), and ethynyldiazonium (**3**) ions and the respective data for their fragmentation products are summarized in Tables I and II, respectively. Structures and vibrational frequencies are available as supplementary material (see the paragraph at the end of the paper regarding supplementary material).

Methyldiazonium Ion. Molecular-model-type drawings[36] of the C_{3v}-symmetric structure, **1a**, and the two bridged structures, **1b** and **1c**, are shown in Figure 1. It is noteworthy that the NN bond is slightly shorter and that the NN-stretching frequency is higher in **1a** compared to free N_2[40] (1.078 Å, $\nu_{NN}(\sigma)$ = 2761.5 cm^{-1}). The geometries of the subsystems in **1b** and **1c** are practically those of the free subsystems. Structure **1a** is the only minimum.

Foster and Beauchamp measured the heat of formation of **1** by ion cyclotron resonance spectroscopy and found $\Delta H_f(\mathbf{1})$ = 223 kcal/mol.[10a] Subsequently, these workers and Williamson measured the photoionization appearance potential of **1** from $CH_3N_2CH_3$ and obtained $\Delta H_f(\mathbf{1})$ = 209.4 kcal/mol.[10b] Combination of their photoionization appearance potential with the latest value for the heat of formation of $CH_3N_2CH_3$,[41] $\Delta H_f(CH_3N_2CH_3)$ = 35.5 kcal/mol, gave $\Delta H_f(\mathbf{1})$ = 212.9 kcal/mol.[11] With $\Delta H_f(CH_3^+)$ = 261.2 kcal/mol,[42] these three $\Delta H_f(\mathbf{1})$ values yield methyl cation affinities for N_2 of 38.2,[10a] 51.2,[10b] and 48.3[11] kcal/mol, respectively.

The RHF binding energies[43] of 28.5[37] (4-31G), 25.5[38] (DZ+P), 26.0[39] (6-31G*), and 21.0 (6-31G* + VZPEs) all are too low. The inclusion of perturbational corrections for electron correlation significantly improve the binding energies (Table II), and they all are within 2.5 kcal/mol of the experimental value of 38.2 kcal/mol determined by ion cyclotron resonance spectroscopy.[10a] A binding energy of 37.3 kcal/mol is found at the level MP4[SDQ]/6-31G*//RHF/6-31G* + VZPEs. The effect of electron correlation on the structure of **1a** has been examined at the levels MP2(full)/6-31G* and MP2(full)/6-311G**. Structural optimizations of **1a** at MP2(full)/6-31G* shortens the CN bond by 0.050 Å and lengthens the NN bond by 0.055 Å, and the structure determined at MP2(full)/6-311G** is only slightly different.[44] At these levels the dediazoniation of **1a** is endothermic by 47.1 kcal/mol (MP2(full)/6-31G*) and 48.0 kcal/mol (MP2(full)/6-311G**), respectively. The correction for the vibrational zero-point energies determined at MP2(full)/6-31G* reduces these values by 5.2 kcal/mol to 41.9 and 42.8 kcal/mol, respectively. Energies at several levels of Møller–Plesset perturbation theory were calculated in the frozen-core approximation with the MP2(full)/6-31G* structures of **1a** and its fragments. The dediazoniation was found to be endothermic by 42.6 and 43.1 kcal/mol at the levels MP4[SDQ]/6-31G* and MP4[SDQ]/6-311G**, respectively, and the inclusion of triple excitations resulted in values of 45.0 kcal/mol (MP4[SDTQ]/6-31G*) and 45.9 kcal/mol (MP4[SDTQ]/6-311G**). With the correction for vibrational zero-point energies determined at MP2(full)/6-31G* our best theoretical estimate of the binding energy of **1a** is 40.7 kcal/mol at the level MP4[SDTQ]/6-311G**/MP2(full)/6-31G* + VZPEs(MP2(full)/6-31G*). This estimate is within the range of the experimental values, but it remains about 8 kcal/mol below the latest experimental value of 48.3 kcal/mol.[11] It is possible that the latest experimental value could be in error by a few kilocalories per mole since photoionization appearance potentials do not always provide reliable heats of formation for ionic species.[11] Further experimental efforts as well as higher level ab initio studies are desirable to clarify this discrepancy.

These results suggest that the computational level selected for the present study is not unreasonable. Correlation effects on structures increase the stability of the methyldiazonium ion, but the correlation effects on the vibrational zero-point energies counteracts and our best estimate for the binding energy of **1a** is only slightly higher than the value determined at MP4[SDQ]/6-31G*//RHF/6-31G* + VZPEs(RHF/6-31G*).

Technically, structure **1b** represents a transition structure (i143.8 cm^{-1} a") and **1c** is a second-order saddle-point structure

(34) Biegler-König, F. W.; Bader, R. F. W.; Tang, T.-H. *J. Comput. Chem.* **1982**, *3*, 317.

(35) (a) Møller, C.; Plesset, M. S. *Phys. Rev.* **1934**, *46*, 1423. (b) Binkley, J. S.; Pople, J. A. *Int. J. Quantum Chem.* **1975**, *9*, 229. (c) Pople, J. A.; Seeger, R. *Int. J. Quantum Chem.* **1976**, *10*, 1. (d) Pople, J. A.; Krishnan, R.; Schlegel, H. B.; Binkley, J. S. *Int. J. Quantum Chem.* **1978**, *14*, 91, 545. (e) Krishnan, R.; Frisch, M. J.; Pople, J. A. *J. Chem. Phys.* **1980**, *72*, 4244.

(36) Basis set effects on structures are small. Compare the structures of **1** optimized with the basis sets STO-3G (ref 37), 4-31G (ref 37), and DZ+P (ref 38).

(37) Vincent, R.; Radom, L. *J. Am. Chem. Soc.* **1978**, *100*, 4306.

(38) Demontis, P.; Ercoli, R.; Gamba, A.; Suffritti, G. B.; Simonetta, M. *J. Chem. Soc., Perking Trans. 2* **1981**, 488.

(39) Ford, G. P. *J. Am. Chem. Soc.* **1986**, *108*, 5104.

(40) *The Carnegie-Mellon Quantum Chemistry Archive*, 3rd ed.; Whiteside, R. A., Frisch, M. J., Pople, J. A., Eds.; Carnegie-Mellon University: Pittsburgh, PA, 1983.

(41) Rossini, F. D.; Montgomery, R. L. *J. Chem. Thermodyn.* **1978**, *10*, 465.

(42) Traeger, J. C.; McMoughlin, R. G. *J. Am. Chem. Soc.* **1981**, *103*, 3647.

(43) The term *binding energy* refers to the stability of the diazonium system with respect to the combined energies of the isolated subsystems. The term is used for all kinds of stationary structures whether they are minima or saddle points.

(44) Structure of **1a** at MP2(full)/6-31G*: CN = 1.4602 Å, NN = 1.1276 Å, CH = 1.0915 Å, HCN = 106.10°, VZPE = 28.73 kcal/mol. Structure of **1a** at MP2(full)/6-311G**: CN = 1.4596 Å, NN = 1.1185 Å, CH = 1.0910 Å, HCN = 105.96°.

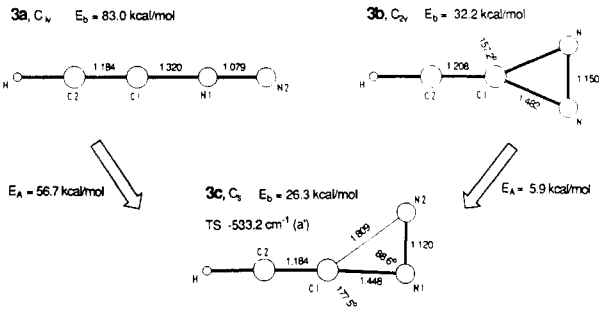

Figure 3. C-sp-attached diazonium function: ethynyldiazonium ion (**3**). In contrast to the automerizations of **1** and **2**, N scrambling in **3a** involves the intermediate **3b** and isomerization between the minima proceeds via the transition-state structure **3c**. Binding energies are with respect to the triplet ground state of ethynyl cation. Compare legend to Figure 1.

(i144.0 cm^{-1} a″ and i26.0 cm^{-1} a″), but **1b** and **1c** are almost isoenergetic and a distinction between their characters therefore becomes irrelevant.[45,46] The important point with regard to these structures is that *automerization of methyldiazonium ion requires virtually complete disconnection and reconnection of dinitrogen* and that *displacements and rotation of the methyl group during automerization are essentially free.* The binding energies of the bridged structures are only 2.8 kcal/mol, and this value might even ben overestimated due to basis set superposition problems[47] in the ion–molecule system.[48]

Vinyldiazonium Ion. We have located the optimal structures of **2** in which the methyne carbon bridges the N_2 unit (Figure 2). Both of these structures a priori are possible transition-state structures for automerization of the planar minimum **2a**.[20,49] Higher level ab initio studies of the parent vinyl cation showed a preference for the bridged nonclassical form over the classical open-chain isomer.[50-52] Nevertheless, binding energies are given here with respect to the classical form. Vinyl cations behave in solution as if they were classical,[16] and ^{13}C NMR studies of vinyl cations[53] provide supporting evidence. It is the intrinsic bonding properties of these intermediates that we are seeking to better understand.

As with **1**, correlation effects significantly increase the binding energies (Table II). At the highest level and with inclusion of vibrational zero-point energies a binding energy of 22.8 kcal/mol is found for **2a**.

The transition vector (i99.8 cm^{-1} a′) identifies **2b** as the transition structure for N scrambling by coplanar N_2 rotation. The structure C_s **2c** technically is a second-order saddle-point structure (i101.9 cm^{-1} a″ and i32.5 cm^{-1} a″). The geometries of the subsystems are essentially those of the isolated vinyl cation and N_2, and the CN distances are in excess of 3.6 Å. The binding energies of **2b** and **2c** are less than 0.8 kcal/mol. Thus, the mechanisms for automerization of **1** and **2** are qualitatively similar.

Ethynyldiazonium Ion. The automerization of the linear minimum[20,21,54] **3a** (Figure 3) differs from the N-scrambling processes of **1** and **2** in two ways. The bridged C_{2v} structure **3b** is a local minimum. The architecture of **3b** allows for a bonding situation whose extremes might conveniently be described as a π-complex between the acceptor HCC^+ ($^1\Sigma^+[\pi^4]$) and the donor N_2 (resonance form I), or as a 2,3-diaza-1-methyniumylcyclopropene (resonance form II). These two resonance forms merely serve to describe whether the in-plane HCC "π"-electrons remain essentially localized or whether they become involved in CN bonding. The geometry clearly favors the description of **3b** as a π-complex. The sp LUMO of HCC^+ greatly increases the acceptor capability relative to methyl and vinyl cations and makes the formation of a π-complex possible. Whereas the bridged structures of **1** and **2** (<2.7 Å) are loose ion–molecule aggregates, the CN bonds in **3b** are short (1.482 Å). The NN and the CC bonds in **3b** both are slightly longer than in **3a** (Table III), but they remain triple bonds indicating that resonance form I prevails. Isomerization between the minima **3a** and **3b** proceeds via the planar transition-state structure **3c** (i533.2 cm^{-1} a′).

The minimum **3a** is 83.0 kcal/mol more stable than the triplet ground state of ethynyl cation and free N_2 (Table II).[55] UHF wave functions are not eigenfunctions of the $\langle S^2 \rangle$ operator, and the structure and energy of the $^3\Pi$ state of ethynyl cation therefore include some contaminations from higher spin states.[56] The annihilation[57] of the quintet and septet spin states effectively removes the spin contaminations, and the total energies of the $^3\Pi$ state and of the binding energies are lowered by 4–5 kcal/mol.[58] **3** is more than twice as stable toward dediazoniation compared to **1** and **2** (Table II), and the kinetic stability is even higher.[20] In marked contrast to **1** and **2**, the *automerization of 3 proceeds within a bound ion–molecule complex* via a π-complex-type intermediate. The local minimum **3b** and the transition structure **3c** are more stable than the isolated subunits by 32.2 and 26.3 kcal/mol, respectively. Again, spin annihilation in the $^3\Pi$ state of ethynyl cation reduces these values by about 4 kcal/mol. The activation barriers for the processes **3a** → **3c** → **3b** and **3b** → **3c** → **3a** are 56.7 and 5.9 kcal/mol, respectively. While the automerizations of **1** and **2** involve *inter*molecular exchange, the automerization of **3** is a largely *intra*molecular process.

Further Discussion. Remarkably, the thermodynamic stability of the vinyldiazonium ion is found to be *lower*[59] than those of the methyl- and ethynyldiazonium ions. The CN distances (**1a**, 1.510 Å; **2a**, 1.434 Å; and **3a**, 1.320 Å) and the frequencies of the

(45) Truhlar, D. G.; Hase, W. L.; Hynes, J. T. *J. Phys. Chem.* **1983**, *87*, 2664.

(46) The transition structure **2c** in ref 37 is isoenergetic as well and needs no further consideration here.

(47) See: Hobza, P.; Zahradnik, R. *Chem. Rev.* **1988**, *88*, 871, and references cited therein.

(48) The low binding energies in combination with the superposition problems causes the large basis set effects on the CN distances in the bridged structures of **1**: 2.118 Å at STO-3G, 2.867 Å at 4-31G, and 2.743 at 6-31G*.

(49) (a) Fols, E.; Gamba, A.; Suffritti, B.; Simonetta, M.; Szele, I.; Zollinger, H. *J. Phys. Chem.* **1982**, *86*, 3722. (b) Fortuitously, the RHF/4-31G binding energy of 19.4 kcal/mol agrees reasonably well with the MP4-[SDQ]/6-31G* value determined here.

(50) (a) Raghavachari, K.; Whiteside, R. A.; Pople, J. A.; Schleyer, P. v. R. *J. Am. Chem. Soc.* **1981**, *103*, 5649. (b) Pople, J. A. *Chem. Phys. Lett.* **1987**, *137*, 10. (c) Lindh, R.; Roos, B. O.; Kraemer, W. P. *Chem. Phys. Lett.* **1987**, *139*, 437.

(51) Similarly, ethynylvinyl cation was shown to favor the nonclassical form compared to the β-ethynylvinyl cation structure at correlated levels: (a) Hori, K.; Yamabe, T.; Tachibana, A.; Asai, Y.; Fukui, K.; Kobayashi, S.; Taniguchi, H. *J. Mol. Struct. (Theochem)* **1987**, *153*, 295. (b) Unpublished results.

(52) Coulomb explosion imaging shows vinyl cation to be nonclassical: Vager, Z.; Naaman, R.; Kanter, E. P. *Science* **1989**, *244*, 426.

(53) (a) Siehl, H.-U.; Mayr, H. *J. Am. Chem. Soc.* **1982**, *104*, 909. (b) Siehl, H.-U.; Koch, E. W. *J. Org. Chem.* **1984**, *49*, 575. (c) Siehl, H.-U. *J. Chem. Soc., Chem. Commun.* **1984**, 635. (d) Koch, E.-W.; Siehl, H. U.; Hanack, M. *Tetrahedron Lett.* **1985**, *26*, 1495.

(54) Correlation effects on structures were examined for **3** in ref 20 and they were found to be small.

(55) The differences between the binding energies determined at the RHF and the highest correlated level are 16.3 (**1a**), 10.5 (**2a**), and 45.0 (**3a**) kcal/mol, respectively. The large value for **3a** primarily reflects the different electron correlation corrections for the $^3\Pi$ and the $^1\Sigma^+(\pi^4)$ states of ethynyl cation (cf. ref 20). The energies for the reaction **3a** → HCC^+, $^1\Sigma^+(\pi^4)$ + N_2 vary less since the electronic structures of the HCC^+, $^1\Sigma^+(\pi^4)$ and of the CC triple bond in **3a** are similar and give comparable contributions to the correlation energy corrections. The energies of ethynyl cation in its $^1\Sigma^+(\pi^4)$ state (based on the RHF/6-31G* structure with CC = 1.173 Å and CH = 1.075 Å) are −75.617 75 (RHF), −75.838 32 (MP2), −75.850 37 (MP3), −75.853 72 (MP4[DQ]), and −75.858 58 (MP4[SDQ]), respectively, and the zero-point-energy corrected (scaled VZPE of HCC^+, $^1\Sigma^+(\pi^4)$ is 10.4 kcal/mol) reaction energies for the process **3a** → HCC^+, $^1\Sigma^+(\pi^4)$ + N_2 are 144.9 (RHF), 162.4 (MP2), 154.2 (MP3), 152.3 (MP4[DQ]), and 152.1 (MP4[SDQ]), respectively. Thus, the difference between these reaction energies determined at the RHF and the highest correlated level is only 7.2 kcal/mol.

(56) Szabo, A.; Ostlund, N. S. *Modern Quantum Theory*; Macmillan: New York, 1982; p 104 ff.

(57) Schlegel, H. B. *J. Chem. Phys.* **1986**, *84*, 4530.

(58) Annihilation of quintets and septets yields $\langle S^2,0 \rangle$ = 2.0 and the energies (in atomic units) PUHF = −75.794 55, PMP2 = −75.949 11, PMP3 = −75.966 76, and PMP4 = −75.977 53.

(59) This conclusion remains qualitatively correct even if the nonclassical structure of vinyl cation were considered for the binding energy. At MP4-[SDTQ]/6-311G**(2df)//MP2(full)/6-31G* the nonclassical structure is preferred over the classical one by 4.6 kcal/mol (see ref 50b).

vibrations that primarily are CN-stretching modes (**1a**, 642.9 cm^{-1} a_1; **2a**, 761.7 cm^{-1} a'; and **3a**, 985.1 cm^{-1} σ) indicate that the CN-bond strengths increase in the order **1a** < **2a** < **3a** (relation I). This ordering can be rationalized by the different Cl hybridizations. The binding energies also are affected by the ability of the hydrocarbon fragment to accommodate positive charge. Ethynyl cation clearly is least suited in this regard.[20] Methyl and vinyl cation both have a p LUMO, but they differ in the hybridization of the remaining C orbitals. The saturated cation has an C-sp^2-σ frame whereas the (formally) electron-deficient center of vinyl cation uses two sp orbitals and one p orbital for bonding. If the Lewis notations were valid representations of the actual electron density distributions, one would conclude that CH_3^+ would accommodate positive charge better than $C_2H_3^+$ because the electronegativity increase of the electron-deficient C atom would stabilize σ bonds more than π bonds. Thus, one would assume that the ability to accommodate a positive charge increases in the order $HCC^+ < C_2H_3^+ < CH_3^+$ (relation II). With relations I and II the binding energies of the diazonium ions would be expected to increase with the degree of unsaturation. The available experimental data also indicate that (substituted) vinyldiazonium ions are rather stable toward dediazoniation whereas alkyldiazonium ions are not (vide supra). This discrepancy between expectations and experimental results on one hand and the presented theoretical results on the other will be resolved by the electron density analysis of the diazonium ions and their subsystems.

2. Topological Electron Density Analysis. The topological analysis is based on the gradient vector field of the electron density, $\nabla\rho(\mathbf{r})$, and on the Laplacian of the density, $\nabla^2\rho(\mathbf{r})$. Excellent reviews on the subject are available,[25] reference to relevant primary literature is made in the tables, and only a brief description of selected topological parameters pertinent to this work is thus required. Subspaces within $\rho(\mathbf{r})$, so-called basins, are defined as regions in 3D space bounded by a zero-flux surface of the gradient vector field of $\rho(\mathbf{r})$, that is, a surface for which $\nabla\rho(\mathbf{r})\cdot\mathbf{n}(\mathbf{r}) = 0$ at all points. Critical points in $\nabla\rho(\mathbf{r})$, points where $\nabla\rho(\mathbf{r}) = 0$, define the principal characteristics of the electron distribution. Pertinent results of the topological analysis of the ions **1**–**3** and their fragmentation products are summarized in Table III. The locations of critical points in $\rho(\mathbf{r})$ are specified by their distances r_A and r_B from the positions of the atoms A and B, and the parameter F as defined in Table III. Each critical point is further characterized by the electron density ρ_b, the eigenvalues λ_i of the Hessian matrix of $\rho(\mathbf{r})$ (the principal curvatures of $\rho(\mathbf{r})$), and the Laplacian $\nabla^2\rho(\mathbf{r}) = \sum\lambda_i$ at its position. Critical points also are classified according to the rank, denoting the number of nonzero eigenvalues λ_i, and the signature, the number of excess positive over negative eigenvalues λ_i.[61] Critical points (3,+3) and (3,−3) usually coincide with the centers of cages and the positions of nuclei, respectively. Critical points (3,+1) and (3,−1) are saddle points and occur in the central position of a ring system or between bonded atoms, respectively. The unique trajectory traced out by $\nabla\rho(\mathbf{r})$, associated with the positive eigenvalue, and originating at the bond critical point defines the bond path, and the trajectories associated with the negative eigenvalues define the zero-flux surface that partitions the molecule into basins. Important properties of such basins are summarized in Table IV. The values reported include atom and fragment populations, N, the contributions to the populations associated with (valence) π MOs, N_π, and atom and fragment energies T'.

In Figures 4–6 the gradient vector fields of the electron densities of the diazonium ions **1**–**3** are plotted. Bond paths and cross sections of the zero-flux surfaces are also drawn. Figure 6 shows

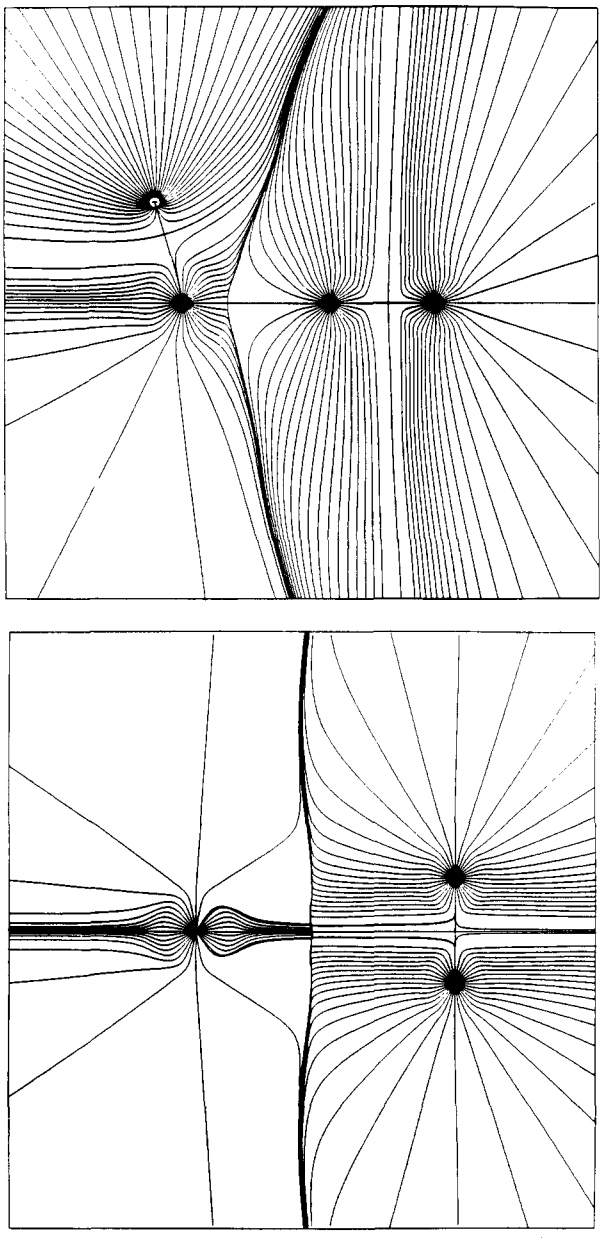

Figure 4. Graphical representations of the gradient vector fields of the electron densities and of the molecular graphs of methyldiazonium ion **1a** (top) and its transition-state structure for automerization **1b**. The gradient paths asymptotically approach the cross sections of the zero-flux surfaces of $\nabla\rho(\mathbf{r})$. These cross sections intersect with the bond paths at bond critical points.

that so-called pseudoatoms occur in the CC-bonding regions of **3a**–**3c** and unusual topological features also are found for ethynyl cation. These features are briefly discussed before we proceed with the analysis of the diazonium ions.

2.1. Occurrence of Pseudoatoms and Pseudocages in CC Triple Bonds. Usually all gradient paths terminate at one of the nuclei; that is, a nucleus acts as an attractors in $\nabla\rho(\mathbf{r})$. The space containing all of the gradient paths that terminate at one and the same nucleus defines the basin, and an ATOM (atom topologically defined for molecules) is defined as the union of an attractor and its basin.[25] Only recently have ATOMs been found that do not contain a nucleus[62] and the associated nonnuclear (3,−3) critical

(60) (a) Bader, R. F. W.; Anderson, S. G.; Duke, A. J. *J. Am. Chem. Soc.* **1979**, *101*, 1389. (b) Bader, R. F. W.; Nguyen-Dang, T. T.; Tal, T. *J. Chem. Phys.* **1979**, *70*, 4316. (c) Bader, R. F. W. *J. Chem. Phys.* **1980**, *76*, 2871. (d) Bader, R. F. W.; Slee, T. S.; Cremer, D.; Kraka, E. *J. Am. Chem. Soc.* **1983**, *105*, 5061. (e) Cremer, D.; Kraka, E.; Slee, T. S.; Bader, R. F. W.; Lau, C. D. H.; Nguyen-Dang, T. T.; MacDougall, P. J. *J. Am. Chem. Soc.* **1983**, *105*, 5069. (f) Bader, R. F. W.; Essen, H. *J. Chem. Phys.* **1984**, *80*, 1943.
(61) Collard, K.; Hall, G. G. *Int. J. Quantum Chem.* **1977**, *12*, 623.

(62) (a) Gatti, C.; Fantucci, P.; Pacchioni, G. *Theor. Chim. Acta* **1987**, *72*, 433. (b) Cao, W. L.; Gatti, C.; MacDougall, P. J.; Bader, R. F. W. *Chem. Phys. Lett.* **1987**, *141*, 380. (c) Pseudoatoms previously described include Be_2, Li_2, and C_2 and their positive ions (ref 25b) and acetylene (ref 60d), and they were thought to be artifacts. (d) Diphosphorus shows a nonnuclear attractor in the RHF, MP2, and CISD densities calculated with several large basis sets including higher angular momentum polarization functions (f orbitals). To be published.

TABLE III: Important Bond Properties of Methyl-, Vinyl-, and Ethynyldiazonium Ions[a]

bond	r_A[b]	r_B	F[c]	ρ_b[d]	λ_1[e,f]	λ_2	λ_3	ϵ[g]
				Methyldiazonium Ion, **1a**				
C N1	0.434	1.053	0.292	0.170	−0.083	−0.083	0.763	0.000
N1 N2	0.586	0.487	0.546	0.690	−1.507	−1.507	0.491	0.000
				Methyldiazonium Ion, **1b**				
C N1	1.196	1.567	0.433	0.011	−0.004	−0.000	0.043	22.849
C N1[h]	1.194	1.590	0.429	0.011	−0.004	−0.000	0.042	
N N	0.541	0.541	0.500	0.710	−1.729	−1.689	0.663	0.024
				Methyldiazonium Ion,[i] **1c**				
N1 N2	0.541	0.541	0.500	0.710	−1.729	−1.688	0.663	0.024
				Vinyldiazonium Ion, **2a**				
C1 N1	0.438	0.997	0.305	0.210	−0.252	−0.232	1.155	0.086
N1 N2	0.599	0.477	0.557	0.681	−1.552	−1.516	0.454	0.023
C1 C2	0.719	0.600	0.545	0.364	−0.820	−0.595	0.150	0.379
				Vinyldiazonium Ion, **2b**				
C1 N1	1.597	1.743	0.478	0.004	−0.002	−0.001	0.018	0.563
N1 N2	0.539	0.540	0.500	0.711	−1.709	−1.694	0.647	0.009
C1 C2	0.827	0.435	0.655	0.386	−0.816	−0.668	0.733	0.223
				Vinyldiazonium Ion, **2c**				
C1 N	1.549	1.858	0.455	0.003	−0.002	−0.001	0.016	0.833
N N	0.540	0.540	0.500	0.711	−1.709	−1.696	0.649	0.008
C1 C2	0.827	0.435	0.655	0.386	−0.817	−0.667	0.733	0.224
				Ethynyldiazonium Ion, **3a**				
C1 N1	0.416	0.904	0.315	0.291	−0.583	−0.583	1.871	0.000
N1 N2	0.623	0.332	0.652	0.668	−1.498	−1.498	0.380	0.000
C1 C2	0.441	0.744	0.372	0.410	−0.637	−0.637	0.517	0.000
C1 C2[j]	0.593	0.591	0.501	0.413	−0.559	−0.559	−0.118	0.000
C1 C2	0.756	0.428	0.639	0.409	−0.456	−0.456	0.660	0.000
				Ethynyldiazonium Ion, **3b**				
C1 N	0.594	0.896	0.399	0.241	−0.475	−0.089	0.236	4.868
C1 N[h]	0.588	0.970	0.377	0.240	−0.467	0.444	0.210	
N N	0.575	0.575	0.500	0.616	−1.641	−1.379	0.924	0.190
C1 C2	0.433	0.775	0.358	0.403	−0.588	−0.480	0.579	0.226
C1 C2[j]	0.657	0.552	0.543	0.408	−0.776	−0.492	−0.064	0.578
C1 C2	0.748	0.460	0.619	0.408	−0.873	−0.465	0.224	0.877
				Ethynyldiazonium Ion, **3c**				
C1 N1	0.488	1.819	0.336	0.238	−0.422	−0.400	0.381	0.055
N1 N2	0.554	0.576	0.486	0.663	−1.818	−1.533	0.854	0.202
C1 C2	0.427	0.758	0.360	0.407	−0.471	−0.408	0.663	0.154
C1 C2[j]	0.582	0.602	0.492	0.411	−0.574	−0.500	−0.128	0.147
C1 C2	0.746	0.438	0.630	0.407	−0.681	−0.559	0.579	0.218
				Nitrogen				
N N	0.539	0.539	0.500	0.711	−1.699	−1.699	0.638	0.000
				Vinyl Cation, Classical				
C1 C2	0.827	0.435	0.655	0.386	−0.817	−0.668	0.734	0.224
				Vinyl Cation, Distorted				
C1 C2	0.816	0.455	0.642	0.375	−0.756	−0.590	0.391	0.281
				Ethynyl Cation, $^1\Sigma^+(\pi^4)$, RHF/6-31G* Density				
C2 C1[k]	0.399	0.774	0.360	0.312	0.114	0.114	1.390	
C2 C1[l]	0.427	0.778	0.354	0.353	−0.231	0.000	0.593	
C2 C1[j]	0.577	0.596	0.492	0.363	−0.230	−0.230	−0.265	
C2 C1	0.743	0.433	0.632	0.356	−0.368	−0.368	0.864	
				Ethynyl Cation, $^1\Sigma^+(\pi^4)$, MP2(full)/6-31G* Density				
C2 C1[k]	0.416	0.805	0.341	0.307	0.144	0.144	0.855	
C2 C1[l]	0.462	0.784	0.731	0.309	−0.277	0.000	0.269	
C2 C1[j]	0.604	0.617	0.495	0.313	−0.194	−0.194	−0.101	
C2 C1	0.757	0.464	0.620	0.311	−0.230	−0.230	0.321	
				Ethynyl Cation, $^1\Sigma^+(\pi^4)$, CISD/6-31G* Density				
C2 C1[k]	0.413	0.807	0.339	0.313	0.114	0.114	0.956	
C2 C1[l]	0.448	0.798	0.360	0.314	−0.233	0.000	0.373	
C2 C1[j]	0.635	0.586	0.519	0.321	−0.248	−0.248	−0.084	
C2 C1	0.751	0.470	0.615	0.320	−0.277	−0.277	0.244	
				Ethynyl Cation, $^1\Sigma^+(\pi^4)$, MP2(full)/6-311++G** Density				
C2 C1[k]	0.447	0.774	0.366	0.312	0.203	0.203	0.176	
C2 C1[l]	0.456	0.768	0.373	0.312	−0.039	0.000	0.134	
C2 C1[j]	0.500	0.721	0.410	0.312	−0.095	−0.095	−0.078	
C2 C1	0.671	0.550	0.550	0.311	−0.259	−0.259	0.070	

TABLE III (Continued)

bond	r_A[b]	r_B	F[c]	ρ_b[d]	λ_1[e,f]	λ_2	λ_3	ϵ[g]
Ethynyl Cation, $^1\Sigma^+(\pi^4)$, CISD/6-311++G** Density								
C2 C1[k]	0.435	0.785	0.357	0.318	0.022	0.022	0.340	
C2 C1[l]	0.442	0.779	0.362	0.318	−0.045	0.000	0.265	
C2 C1[j]	0.541	0.679	0.443	0.319	−0.184	−0.184	−0.054	
C2 C1	0.639	0.582	0.523	0.318	−0.274	−0.274	0.038	

[a] Electron density analysis at RHF/6-31G* unless otherwise specified. All correlated electron densities of HCC^+ are based on the MP2(full)/6-31G* structure. See Figures 1–3 for atom numbering. [b] Distance r_A (r_B) of atom A (B) from the bond critical point in Å. [c] The distance of the bond critical points (BCP) from atom A is given by the fraction F of the bond length d(AB); $F = r_A/(r_A + r_B)$. [d] Density at the critical point ρ_b (in e au^{-3}). [e] Eigenvalues λ_i of the Hessian matrix **A** of $\rho(\mathbf{r})$ at the critical point (in e au^{-5}); see ref 60a–c. [f] The Laplacian $\nabla^2(\rho)$ at the critical point is the defined as $\nabla^2(\rho) = \sum\lambda_i$ (in e au^{-5}); cf. ref 60d,f. [g] Bond ellipticity ϵ, defined as $\epsilon = \lambda_n/\lambda_m - 1$, where $\lambda_n < \lambda_m$ and $\lambda_i < 0$ ($i = n, m$); cf. ref 60d,e. [h] Position of a (3,+1) ring critical point. [i] The position of the CN bond critical point could not be determined accurately due to the small curvature of the electron density. [j] Position of a pseudoatom or nonnuclear attractor; $\lambda_i < 0$ for all i. Cf. ref 62. [k] *Pseudocage point* on the CC axis; all $\lambda > 0$. [l] Radii of (2,0) critical rings concentric around the CC axis where $\lambda_1 < 0$, $\lambda_2 = 0$, and $\lambda_3 > 0$: RHF/6-31G* 0.131 Å, MP2(full)/6-31G* 0.120 Å, CISD/6-31G* 0.119 Å, MP2(full)/6-311++G** 0.028 Å, CISD/6-311++G** 0.041 Å.

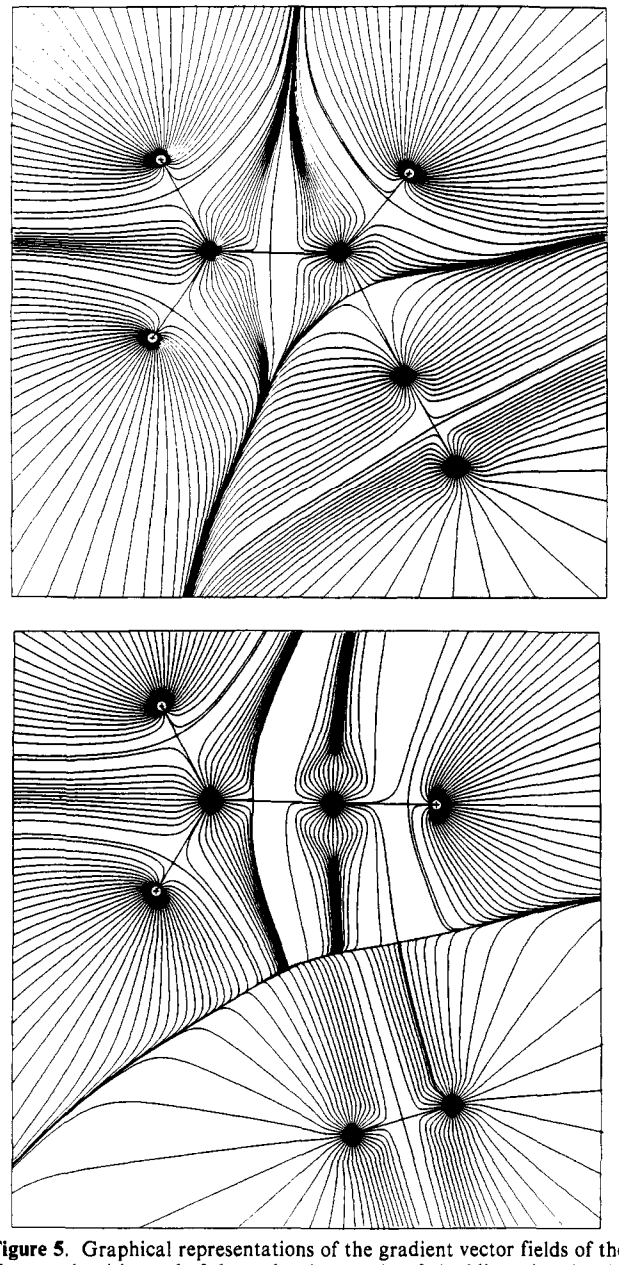

Figure 5. Graphical representations of the gradient vector fields of the electron densities and of the molecular graphs of vinyldiazonium ion **2a** (top) and its transition-state structure for automerization **2b**. Compare legend to Figure 4.

points are referred to as pseudoatoms. The unique trajectories traced out by $\nabla\rho(\mathbf{r})$, associated with the eigenvalues λ_3, and originating at each of the pseudoatoms define bond paths between the pseudoatoms and the adjacent C atoms. The differences between the ρ values at the locations of the pseudoatom and their adjacent bond critical points are marginal. In the case of **3a**, for example, the ρ value at the nonnuclear (3,−3) critical point is 0.413 e au^{-3} and the ρ values at the bond critical points are 0.410 and 0.409 e au^{-3}, respectively. Whether the pseudoatoms in multiply bonded systems are reduced or vanish[62c] or whether they persist[62d] when more complete basis sets are used and/or when correlation effects are taken into account, their occurrence points up a significant problem: The bond critical points are relatively far away from the pseudoatoms. In **3a** these distances are 0.152 and 0.163 Å, and similar distances are found for **3b** and **3c** (Table III). The important point then is that the electron density distributions in the central bonding regions of the CC triple bonds are nearly cylindrical over a wide range. Thus, *the results of topological analyses of multiply bonded systems with nearly cylindrical electron density distributions in the bonding regions might be severely affected by the choice of basis set even if pseudoatoms are absent.* For example, atomic volumes and populations are rather sensitive to small (basis set related) shifts of the partitioning surface since ρ values are comparatively large in the centers of multiple bonds.[63]

Pseudoatoms also have been found in the RHF/6-31G* electron density of ethynyl cation in its $^1\Sigma^+(\pi^4)$ state. While the pseudoatoms in **3a–3c** all are connected to *two* adjacent bond critical points, only one such bond critical point occurs between the pseudoatom and the HC carbon (C2). Between the nonnuclear (3,−3) critical point and C1 a (3,+3) or *pseudocage* critical point occurs instead. This topological feature consisting of two attractors linked by bonded cones has a precedent in the topology of the lowest excited II state of Li_2^+.[25b] The trajectories of $\rho(\mathbf{r})$ which originate at this pseudocage point and define a portion of the partitioning surface between the basins terminate at a ring of (2,0) critical points that encircles the axis. Again, it is emphasized that these unusual topological features are caused by very small differences of $\rho(\mathbf{r})$ in the CC-bonding region. The data collected in Table III show that the ρ value at the location of the pseudoatom is 0.363 e au^{-3} and that the $\rho(\mathbf{r})$ values are only slightly smaller at the bond critical point (by 0.007 e au^{-3}), the (2,0) critical points (by 0.010 e au^{-3}), and the pseudocage point (by 0.051 e au^{-3}). For ethynyl cation electron density analyses have also been carried out at correlated levels of theory. The electron densities calculated at the levels MP2 and CISD with the 6-311++G** basis set and with the MP2(full)/6-31G* geometries still show the described topology *but the differences between the associated $\rho(\mathbf{r})$ values are practically nil* (Table III). At the pseudoatoms the λ_3 values only are −0.078 and −0.054, respectively, and these small curvatures dramatically illustrate the significant problems associated with the partitioning of multiple bonds with nearly cylindrical electron density distributions in the bonding regions. In bonding situations characterized by larger curvatures λ_3 (e.g., >0.3) basis set quality and effects of correlation appear to affect the results of topological density analysis to a small extent only. In contrast, the results presented strongly suggest that higher computational

(63) For a related discussion, see: Glaser, R. *J. Comput. Chem.* **1989**, *10*, 118.

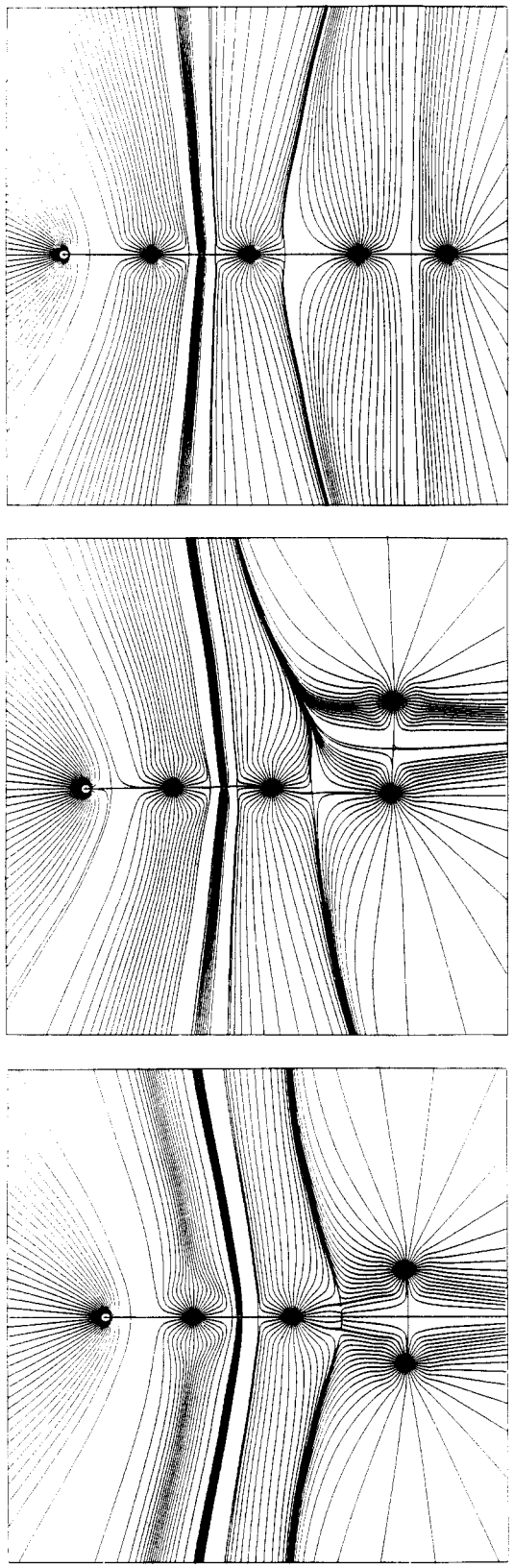

Figure 6. Graphical representations of the gradient vector fields of the electron densities and of the molecular graphs of the global minimum of ethynyldiazonium ion **3a** (top), of the local minimum **3b** (bottom), and the transition-state structure for isomerization **3c**. The electron densities calculated for **3a–3c** all show pseudoatoms to occur in the CC-bonding regions.

levels are required to assure a meaningful partitioning of triply bonded systems with small λ_3 values.

2.2. Bonding in Diazonium Ions. Each ATOM is characterized by the zero-flux surfaces that define its basin and by the electron density distribution therein. Results of density integrations over

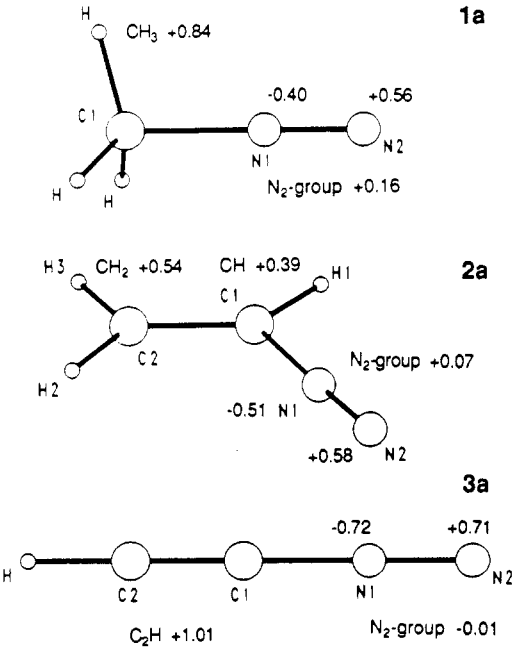

Figure 7. Atom and fragment populations for methyldiazonium (**1a**), vinyldiazonium (**2a**), and ethynyldiazonium (**3a**) ions as obtained by integration within the basins of the RHF/6-31G* electron density distributions.

the basin[64] reflect these characteristics fully, they are rigorously defined, and they precisely describe the *consequences of bonding* on properties of the ATOMs. Bonding itself usually is described within the topological method by specification of the location of critical points and their properties. It is emphasized that bonding is a three-dimensional phenomenon and that this description of bonding based on critical points alone basically is empirical in nature. A rigorous comparison of bonding situations would have to involve comparisons between the three-dimensional gradient vector fields and the Laplacian distributions. Such comparisons can be made qualitatively by use of graphical representations, and more quantitative methods are being explored.[60f,65]

Topological Properties. In Figures 4–6 the zero-flux surfaces are illustrated that partition the CN- and the NN-bonding regions of molecules **1a**, **2a**, and **3a**. It is immediately obvious that both of the partitioning surfaces are shifted away from the N(C) nitrogen (N1) in all cases. The F_{CN} values, defined as $F_{CN} = r_C/(r_C + r_N)$, are 0.292, 0.305, and 0.315 for **1a**, **2a**, and **3a**,[66] respectively. The C basin covers roughly 30% of the CN-bonding region. The CN-ρ_b values (in e au^{-3}) are 0.170 (**1a**), 0.210 (**2a**), and 0.291 (**3a**), and they reflect the increase of the CN-stretching frequencies with the degree of unsaturation (cf. relation I). The λ_3 values are all larger than 0.75, and integrations should thus yield reliable results. The displacements of the NN-bond critical points toward the terminal nitrogens (F_{N1N2} 0.546 for **1a**, 0.557 for **2a**, and 0.652 for **3a**) and the accompanying small decreases (<6%) of ρ_b compared to free N_2 indicate internal N_2 polarizations that increase the N1 populations, and they indicate radial expansion of the density in the NN-bonding regions. The latter is reflected in the curvatures λ_1 and λ_2 at the NN-bond critical points; these values are less negative compared to free N_2. The radial expansion greatly decreases λ_3(NN) in **1a–3a** relative to

(64) The significance of integrated Bader population has been challenged because the atomic charges seemed inconsistent with the dipole moments. This challenge has been answered; see: Bader, R. F. W.; Larouche, A.; Gatti, C.; Carroll, M. T.; MacDougall, P. J.; Wiberg, K. B. *J. Chem. Phys.* **1987**, *87*, 1142.

(65) Compare: Cremer, D.; Kraka, E. *Croat. Chem. Acta* **1984**, *57*, 1259.

(66) We showed that a meaningful partitioning of the CC triple bonds in **3** is impeded because of the nearly cylinder-symmetrical electron density distribution in the CC-bonding regions. The electron density distributions in the CN- and NN-bonding regions are not significantly affected by small changes in the CC bonds, and therefore, the topological analysis of the CN linkage and of the diazo function remains valid.

TABLE IV: Atom Properties of Methyl-, Vinyl-, and Ethynyldiazonium Ions[a]

atom[b]	N_π[c,d]	N[d]	T[e]	atom[b]	N_π[c,d]	N[d]	T[e]
			Methyldiazonium Ion, **1a**[f]				
C	1.063	5.736	37.718 47	H′	0.153	0.808	0.538 80
N1	1.237	7.397	54.877 29	Σ	4.001	22.001	148.216 03
N2	0.831	6.443	54.003 89	N_2	2.068	13.839	108.881 18
H	0.564	0.808	0.538 80	CH_3	1.933	8.161	39.334 85
			Vinyldiazonium Ion, **2a**				
C1	1.143	5.834	37.723 37	H3	0.012	0.817	0.539 97
N1	1.283	7.509	54.979 02	Σ	4.000	27.999	186.059 54
N2	0.884	6.424	53.956 09	N_2	2.167	13.933	108.935 11
H1	0.018	0.780	0.524 38	CH	1.161	6.613	38.247 75
C2	0.648	5.797	37.786 96	CH_2	0.672	7.453	38.876 68
H2	0.012	0.839	0.549 76				
			Vinyldiazonium Ion, **2b**				
C1	1.370	6.559	38.282 05	H3	0.010	0.720	0.479 30
H1	0.010	0.604	0.432 13	N_2[g]	2.000	13.985	108.850 43
C2	0.599	5.416	37.509 22	CH	1.380	7.163	38.714 18
H2	0.010	0.716	0.468 34	CH_2	0.619	6.852	38.466 86
			Ethynyldiazonium Ion, **3a**				
C1	0.889	4.829	37.127 69	H	0.006	0.644	0.450 18
C1 + PA[h]	0.933	6.520	38.204 14	Σ	4.000	26.000	184.797 40
N1	1.367	7.718	55.193 62	N_2	2.172	14.007	109.015 16
N2	0.805	6.290	53.821 55	PA[h]	0.044	0.309	1.076 45
C2	0.610	5.099	37.261 74	C_2H	1.549	12.263	75.916 06
			Ethynyldiazonium Ion, **3b**				
C1[g]	0.738	4.754	37.272 80	H	0.009	0.618	0.437 13
N	1.001	7.056	54.403 67	N_2	2.001	14.112	108.807 34
C2	0.951	5.295	37.382 56	PA[h]	0.301	1.221	0.812 01
C2 + PA[h]	1.252	6.516	38.194 57	C_2H	1.999	11.888	75.904 50
			Ethynyldiazonium Ion, **3c**				
C1	0.679	5.103	37.252 98	H	0.007	0.647	0.451 06
C1 + PA[h]	1.034	6.541	38.212 55	Σ	3.998	25.988	108.703 00
N1	0.985	7.128	54.595 26	N_2	2.050	13.805	108.835 81
N2	1.065	6.677	54.240 55	PA[h]	0.355	1.438	0.959 38
C2	0.907	4.995	37.203 78	C_2H	1.948	12.183	75.867 19
			Methyl Cation				
C		5.855	37.747 84	Σ		8.000	39.230 53
H		0.715	0.494 23				
			Vinyl Cation				
C1	1.370	6.545	38.237 79	Σ	2.000	13.999	77.086 84
H1	0.010	0.605	0.431 54	CH	1.380	7.150	38.669 32
C2	0.599	5.415	37.462 66	CH_2	0.620	6.849	38.417 51
H2	0.010	0.717	0.477 43				
			Vinyl Cation, Distorted				
C1	1.314	6.435	38.101 12	H3	0.010	0.713	0.482 99
H1	0.012	0.627	0.437 83	Σ	2.001	14.002	77.021 30
C2	0.651	5.501	37.518 84	CH	1.326	7.062	38.538 95
H2	0.014	0.726	0.480 52	CH_2	0.675	6.940	38.482 35

[a] At RHF/6-31G*//RHF/6-31G*. [b] See Figures 1–3 for numbering. [c] N_π represents the contribution to N due to the π-symmetric valence MOs. [d] Atomic populations N and N_π in electrons. [e] Integrated atomic kinetic energy corrected for the virial defect of the wave function, T', where $T' = T[-(V/T) - 1)]$. Differences between the sum T'' of the integrated kinetic energies T' and the total energy of the molecule ($-E_{mol} = T_{mol}$), $T'' + E$ in atomic units: **1a** −0.00003; **2a** +0.00019; **3a** +0.00035; **3c** −0.00011; CH_3^+ −0.00011; $C_2H_3^+$ (classical) +0.00010; $C_2H_3^+$ (distorted) −0.00105. [f] N_π values associated with the electron MOs in the HCNN plane. The N_π values associated with the orthogonal electron MOs are C 1.064, N1 1.237, N2 0.831, H 0.016, H′ 0.427, Σ 4.002, N_2 2.068, and CH_3 1.934. [g] By difference. [h] Pseudoatom or nonnuclear attractor.

N_2, but the curvatures remain of such magnitude that the partitioning of the NN-bonding region should be of acceptable quality.

Population Analysis. In Figure 7 pertinent population data are collected for **1a**, **2a**, and **3a**. *The population data show that it is the hydrocarbon fragment that carries most of the positive charge and not the N_2 group.* Transfer of electron density from the diazo function to the positively charged hydrocarbon fragment amounts to only 0.16 electron for **1a**, and it is even smaller for **2a** (0.07) and **3a** (−0.01). The major consequences of the association of a carbenium ion with N_2 on the electron density distribution within the N_2 basin are strong internal polarization and a radial expansion of the density in the NN-bonding region, but only little charge transfer. The population data indicate internal charge transfer on the order of 0.5 electron for **1a** and **2a** and of 0.7 electron for the ethynyl derivative **3a**.

The topological method gives an entirely different account of the electronic structures of diazonium ions compared to the frequently used Mulliken analysis. Mulliken populations greatly underestimate the N_2 populations while they do correctly show that the terminal nitrogen carries a significant positive charge. For example, Mulliken populations of +0.337 (H), −0.376 (C), −0.048 (N1), and 0.413 (N2) were reported for **1a** based on the DZ+P wave function.[38] In the Mulliken scheme overlap populations are equally divided between the bonding partners, and the method therefore intrinsically does not account sufficiently for bond polarities.[67] The topological analysis shows that the CN-

(67) Compare: (a) Gronert, S.; Glaser, R.; Streitwieser, A., Jr. *J. Am. Chem. Soc.* **1989**, *111*, 3111. (b) Bachrach, S. M.; Streitwieser, A., Jr. *J. Comput. Chem.* Submitted for publication.

bond critical points of **1a–3a** are all closer to the C atoms. The density integration approach to populations reflects this feature, but the Mulliken analysis apparently does not. Consequently, the Mulliken population of N1 is underestimated and that of carbon is overestimated.

CN-Bonding Model. The mechanisms by which CN bonding is mediated in **1a**, **2a**, and **3a** can be described by a model that involves σ-donation of electron density from N_2 to the carbenium ion which is accompanied and synergetically enforced by π-back-donation of about equal magnitude. Density accumulation in the CN-bonding region occurs without significant overall charge transfer. The population data in Table IV allow for quantification of these components; $N_\pi(N_2)$ provides a measure for π-back-donation and $N_\sigma(N_2)$ ($N_\sigma = N - N_\pi$) specifies the amount of σ-donation. In **1a** hyperconjugative π-back-donation results in an N_2 population of 2.068 electrons for each set of e-MOs; that is, the overall π-back-donation amount to 0.136 electrons. With the overall N_2 charge of +0.161 the electron density transfer from N_2 to the CH_3 group by σ-donation is thus 0.297 electrons. For the vinyldiazonium ion **2a** the σ-donation of 0.234 electrons from the N_2 group is partially offset by π-back-donation of 0.167 electrons, resulting in the total N_2 charge of +0.067. For **3a** a much larger degree of π-back-donation (0.344 electrons) is found, and this shift of electron density from the HCC fragment into the degenerate π^* MOs of N_2 is larger than the σ-dative electron density transfer in the opposite direction (0.337); thus N_2 carries a small negative charge of −0.007 in **3a**.

The usual Lewis notations are inadequate since they imply transfer of electron density from N_2 to the hydrocarbon fragment and electron depletion at N_α. The proposed bonding model seems more appropriate, and only this model is compatible with the properties of the electron density distributions in the diazonium ions. CN bonding is attributed to the combined stabilization resulting from electron density accumulation in the CN-bonding region and from the electrostatically favorable *quadrupolar* charge distribution in the diazonium ions.

Electronic Reorganization during Automerization. The properties of the gradient vector field of the electron density and the population data of **3b** support the structural argument in favor of resonance form I. The analysis of a series of three-membered rings formed by an acceptor X with ethene (donor A_2) showed that the shape of the AX bond paths reflects the degree of back-donation.[68] Convex or concave bond paths indicate prevailing or moderate π-back-donation, respectively. Accordingly, the concave shapes of the CN bond paths in **3b** (Figure 6) show the dominance of resonance form I. In **3b** the σ-donation involving the in-plane a_1-π MO of the basal N_2 group and the a_1-sp LUMO of HCC^+ ($^1\Sigma^+(\pi^4)$) is enforced by simultaneous back-bonding between the b_2-symmetric in-plane CC-π MO and the appropriate b_2-π^* MO of N_2. Overall N_2 is a stronger π^*-acceptor than it is a σ-donor of π-density; complex formation results in an N_2 charge of −0.112. The resulting strong CN bonding is reflected in the CN-ρ_b values (0.241 e au^{-3}). The fact that **3b** is less stable than **3a** despite these strong CN contacts emphasizes the importance of the stabilization of **3a** by internal N_2 polarization. The translatory motion of the HCC fragment parallel to the NN axis in going from **3b** to the transition-state structure **3c** necessitates a reduction of the overlap required for π-back-donation. Consequently, the CC bond in **3c** is shorter than in **3b** and N_2 is positively charged (+0.195) in **3c**. In **3c** only one CN bond path remains. The equivalence of the molecular graphs of **3c** and **3a** shows that not only the transition state but also the discontinuous change in the molecular graph during isomerization **3b** → **3a** occurs early.

The bridged transition-state structures **1b** and **2b** are topologically distinct. The automerization of **2** proceeds from one open molecular graph to the other without an intermediate ring molecular graph. In **1b** bond paths exist between each of the N atoms and the C atom. The molecular graphs of **3b** and **1b** are similar, but the CN bond paths are much more concave in the latter: The CN bond and the ring critical points are in close proximity with almost identical ρ values, as reflected by the large ϵ value. **1b** is on the verge of changing its ring topology into the open molecular graph associated with **1a** by coalescence of either one of the CN-bond critical points with the ring critical point. Thus, the automerizations of **1–3** are individually distinct with regard to the topological and energetic stabilities of the ring structures **1b–3b** in that **3b** is topologically and energetically stable, **1b** still is topologically (little) stable but energetically unstable, and **2b** is topologically and energetically unstable.

2.3. Electronic Structure of Vinyl Cations. The population analysis of the classical vinyl cation assigns, surprisingly, a charge of −0.15 to the CH group and a charge of +1.15 to the CH_2 fragment. The σ- and π-components of the populations indicate that roughly two-thirds of the CC-π-density are localized at the CH moiety and that a shift of σ-density from the CH_2 to the CH group also occurs. The formation of the CN bond in the vinyldiazonium ion **2a** causes delocalization of the π-density in the C_2H_3 fragment. In **2a** the charges of the CH and CH_2 groups are +0.39 and +0.54, respectively. The shift of π-density from C1 to C2 reflects the reduced electronegativity of C1 in **2a**, and it serves to maximize the electrostatic attraction between the "carbenium ion" and the induced dipole of the N_2 group. Thus, the lower thermodynamic stability of the parent vinyldiazonium ion as compared to methyldiazonium ion can be attributed primarily to the special stabilization of the vinyl cation associated with this reorganization of its electronic structure.[69]

A planar distorted structure of vinyl cation was optimized in which the C2–C1–H1 angle was constrained to 120°. The structure thus obtained is 33.8 kcal/mol higher in energy at the MP4[SDQ]/6-31G*//RHF/6-31G* level than the classical C_{2v} structure. The topological characteristics of the electron density distributions of these two structures are quite similar, and in particular, the charges of the CH and the CH_2 groups of the distorted structure differ by no more than 0.09 from those of the classical structure. The distorted structure is less stable because of changes in the electron density *distribution* in the CH basin, not because of changes in the overall population. Thus, the special stabilization of vinyl cation is due to electron density accumulation at the "sextet" C1 carbon *and* concomitant stabilization of σ-density associated with the change from C1-sp^2 to C1-sp hybridization.

A series of β-(di)substituted vinyl and vinyldiazonium cations have been studied[70] to learn whether the remarkable results obtained for the parent system carry over to these substituted systems and to study the consequences on the endothermicities of the dediazoniations. The CC-π-density localization at the CH carbon is even more pronounced when overall electron-withdrawing substituents (halogens, OH, NH_2) are present in the β-position(s) of vinyl cations. The response of the CC-π-system to strong substituent-induced electron *depletion* at the C2 carbon (charge > +1.5) is *not* counteraction. Electron depletion at C2 together with concentration of electron density at C1 and the β-substituent(s) appears favored (electrostatically) and (Y-) conjugative delocalization is unimportant. The equilibrium geometries of β,β-dihydroxy- and β,β-diaminovinyl cations provide compelling *structural evidence* in support of the results of the topological density analysis. Both of these "onium-carbene-type" structures contain a *nonlinear* CCH fragment; that is, the localization of the "CC-π-density" is complete and causes the CH carbon to assume sp^2 hybridization. In the corresponding diazonium ions the electron depletion at C2 is reduced because of CC-π bonding. Nonetheless, in contrast to the parent vinyldiazonium ion, C2

(68) Cremer, D.; Kraka, E. *J. Am. Chem. Soc.* **1985**, *107*, 3800.

(69) The populations of **2b** (Table IV) show that the electronic structure of the hydrocarbon fragment in **2b** is comparable with the one in the free vinyl cation as opposed to the one in **2a**. This result supports the conclusion that electronic reorganization within $C_2H_3^+$ associated with CN-bond formation is an energy-consuming process. The presence of a distant nitrogen molecule does not suffice to affect this change.

(70) (a) Glaser, R.; Wiberg, K. B. *Abstracts of Papers*, 196th Meeting of the American Chemical Society, Los Angeles; American Chemical Society: Washington, DC, 1988. (b) Glaser, R.; Wiberg, K. B. Manuscript in preparation.

remains greatly electron deficient and the overall positive charge of the carbon skeleton exceeds +1. These results explain the C2-S_N2t-type chemistry and the higher endothermicity of the dediazoniations of these systems. The C2 electrophilicity is a direct consequence of the C2 charge. The increased endothermicity of the dediazoniation (40–60 kcal/mol[70]) indicates that CN bonding benefits more from the increased positive charge of the carbon skeleton than is gained by the localization of the "CC-π-density" at C1 in the free (di-)substituted vinyl cation.

3. Implications. Incipient Nucleophilic Attack. In crystal structures of diazonium ions that contain a proximate nucleophile it was found that the N_2 group is bent in a way that suggested an incipient attack of that nucleophile on N_α with an attack angle of 104°.[71,72] The distortion in 3-carboxy-2-naphthalenediazonium bromide was regarded as the result of attractive interactions between N_α and the carbonyl oxygen and between N_β and the counterion.[71] Similarly, the distortions in the tetrafluoroborate of quinoline-8-diazonium 1-oxide were attributed to an attractive interaction between the O nucleophile and N_α.[72] The results of the topological electron density analysis suggests that the distortions are the result of optimal approach of the nucleophile to the positively charged C atom to which the diazo function is attached and that this approach occurs *despite* the repulsive interaction between the negatively charged N_α and the proximate nucleophile. In both of the crystal structures the N_2 groups are displaced *away* from the nucleophile and this feature is only accounted for by the latter explanation. In fact, these features together with the orientation of N_β toward the gegenion suggest that the electron density distributions of the CN_2 fragments are rather similar to the ones discussed in this study.

Heterosubstituted Diazonium Ions. It appears unlikely that π-back-donation would suffice to compensate for the increased electronegativity of X in the (known) heteroanalogues $[X-N_2]^+$ (X = F, OH, OR, NH_2, ...)[73] of methyldiazonium ion. In contrast to the alkyldiazonium ions, these hetero derivatives migh actually be *azonium* ions, that is, cations in which nitrogen carries the major part of the positive charge.

Diphosphonium Cations. The importance of internal N_2 polarization for CN bonding suggests that the P analogues of diazonium ions might be stable molecules. Diphosphonium ions, $[RP_2]^+$, apparently have not been previously described nor have they been discussed theoretically. Phosphorus is more polarizable than nitrogen and, assuming that the electrostatic charge–dipole interaction remains significant,[74] one might expect diphosphonium ions to be just as or even more thermodynamically stable than diazonium ions. Preliminary results indeed show that methyl- and ethynyldiphosphonium ions are thermodynamically stable with respect to loss of P_2 (even if the dimerization of P_2 is taken into account), and they are more stable in this regard than are the diazonium ions with respect to dediazoniation. The binding energies calculated for methyldiphosphonium ion (C_{3v}) and for the most stable isomer of ethynyldiphosphonium ion (C_{2v}) are 60.6 and 142.2 kcal/mol, respectively, at MP4[SDQ]/6-31G*//RHF/6-31G* + VZPEs(RHF/6-31G*).[2] Elemental phosphorus consists of tetrahedral P_4 molecules in the solid state (white P), the liquid, and the gas phase. Measurable dissociation into P_2 occurs in vapor above 800 °C, but only recently has it been possible to stabilize diphosphorus in transition-metal complexes.[75] Diphosphonium cations potentially provide for a new way of stabilizing P_2, and they might be accessible by direct alkylation of white phosphorus if the thermodynamic stability of the diphosphonium ion were to overcompensate the energy required for the loss of P_2 from the initially formed tetraphosphonium ions.

Conclusions

The stabilities of the diazonium ions depend on the degree of unsaturation in an unexpected way; the binding energies increase in the order **2a** < **1a** < **3a**. The bridged structures **1b**–**3b** along the pathways to automerization are topologically and energetically stable (**3b**), topologically stable but energetically unstable (**1b**), or topologically and energetically unstable (**2b**). The automerizations of **1** and **2** involve virtually complete disconnection, rotation, and reconnection of N_2. In contrast, N scrambling in **3** proceeds within a bound ion–molecule complex via a two-step process in an intramolecular fashion.

Populations determined by electron density integration show that N_2 carries only a *small* positive charge in the diazonium ions.[76] Electron density accumulation in the CN-bonding region, strong internal polarization of N_2, and radial expansion of the density in the NN-bonding region are common features of the (most stable) minima of **1**–**3**.

A bonding model has been proposed for the diazonium ions in which CN bonding is mediated via σ-donation from the diazo function to the "carbenium ion" and synergetic π-back-donation of comparable magnitude. Both the electron density accumulation in the CN-bonding region and the electrostatic attraction between the positive charge of the hydrocarbon fragment and the induced dipole moment of N_2 are important for CN bonding. This bonding model is compatible with the results of the topological analysis. Lewis notations are inconsistent with the electronic structures of the diazonium ions.

The analysis of the electronic reasons for the unexpected ordering of the binding energies, **2a** < **1a** < **3a**, has revealed, surprisingly, that the CC-π-density of the classical vinyl cation is largely localized at the CH group and that the CH_2 group carries a large positive charge. Similar electronic structures occur in β-(di)substituted vinyl cations, and in a few cases, they are manifested in "onium-carbene-type" geometries with nonlinear CCH fragments. The lability of **2**, the higher stability of β-(di)substituted alkenyldiazonium ions, and the C_β-S_N2t-type chemistry of the latter all have been consistently explained with the results of the electron density analysis of the vinyl cations.

The electron density distributions of **1a**–**3a** offer a new and more fully consistent explanation for distortions in the crystal structures of diazonium ions with proximate nucleophilic groups. Extrapolation from the CN-bonding model suggests that heterosubstituted diazonium ions might actually be *azonium* ions. More importantly, the electronic structure analysis suggests the possibility of stabilizing P_2 in diphosphonium ions. Further studies of these and related aspects are in progress.

Acknowledgment. I am indebted to Professors Andrew Streitwieser and Kenneth B. Wiberg for their generosity in providing their computational facilities for this research. This work was supported by NSF Grant CHE85-02137 (A.S.J.) and by a grant from the Exxon Research Foundation (K.B.W.). R.G. was a predoctoral fellow of the Verband der Chemischen Industrie 1985–7.

Registry No. **1**, 20404-06-2; **2**, 64709-62-2; **3**, 108561-02-0; N_2, 7727-37-9; CH_3^+, 14531-53-4; $C_2H_3^+$, 14604-48-9; HCC^+, 16456-59-0.

Supplementary Material Available: Structural parameters and vibrational frequencies of stationary structures of **1**–**3** (Tables V–VIII), an extended version of Table III that includes the topological characterization of the CH bonds (10 pages). Ordering information is given on any current masthead page.

(71) Gougoutas, J. Z.; Johnson, J. *J. Am. Chem. Soc.* **1978**, *100*, 5816.
(72) Wallis, J. D.; Dunitz, J. D. *J. Chem. Soc., Chem. Commun.* **1984**, 671.
(73) Laali, K.; Olah, G. A. *Rev. Chem. Intermed.* **1985**, *6*, 237.
(74) Charge transfer from the diphospho function to the hydrocarbon fragment would undoubtedly be more pronounced than in the diazonium ions, and π-back-donation would no longer be of about the same magnitude compared to σ-dative bonding. Studies of the electronic structures are in progress.
(75) (a) Campana, C. F.; Vizi-Orosz, A.; Palyi, G.; Marko, L.; Dahl, L. F. *Inorg. Chem.* **1979**, *18*, 3054. (b) Scherer, O. J.; Sitzmann, H.; Wolmershäuser, G. *J. Organomet. Chem.* **1984**, *268*, C9. (c) Scherer, O. J.; Sitzmann, H.; Wolmershäuser, G. *Angew. Chem., Int. Ed. Engl.* **1985**, *24*, 351. (d) Schäfer, H.; Binder, D.; Fenske, D. *Angew. Chem., Int. Ed. Engl.* **1985**, *24*, 522.
(76) The charge on the diazo function remains small even in diazonium dications such as cyclopropeniumyldiazonium dications: Glaser, R. *J. Comput. Chem.* Submitted for publication.